Energy loss of electrons traveling parallel to the interface of a semi-infinite granular composite

Carlos I. Mendoza and Rubén G. Barrera
Instituto de Física, Universidad Nacional Autónoma de México, Apartado Postal 20-364, 01000 México D.F., Mexico

Ronald Fuchs
Ames Laboratory and Department of Physics and Astronomy, Iowa State University, Ames, Iowa 50011
(Received 15 August 1997)

The energy loss of an electron traveling above a semi-infinite granular composite consisting of randomly located spherical inclusions is investigated. We express this loss in terms of a surface response function which is then calculated using an effective medium theory for the bulk dielectric function of the system. Three different models are analyzed. The first two models correspond to local and nonlocal versions of a truncated bulk, and the third one includes the effects of the distribution of the spherical inclusions near the surface. We find that a correct treatment of this distribution is necessary in order to get meaningful results. [S0163-1829(98)03618-2]

I. INTRODUCTION

Electron energy-loss spectroscopy of high-energy electrons is becoming an important tool for structural analysis of inhomogeneous materials. Extremely narrow beams of electrons with energies of the order of 100 KeV are produced in scanning transmission electron microscopes (STEM) and their energy loss is measured after passing through a thin sample.[1,2] Here we are interested in granular materials and in the excitation of valence electrons, which means energy losses from a few eV to less than 100 eV. In this energy range a dielectric approach becomes appropriate and the concept of an effective medium with an effective dielectric response has been recently developed and successfully applied to a model of identical spherical inclusions in an otherwise homogeneous matrix.[3–5] In this theory the energy-loss function is given in terms of an effective nonlocal dielectric response which is then calculated in the mean-field approximation. Here we pose a related problem: the calculation of the energy loss of electrons traveling close and parallel to the interface of a semi-infinite system of random spherical inclusions. Since the trajectories of electrons can be controlled very precisely, it is now possible to direct a narrow beam of electrons so it travels a few angstroms away from the surface of a flat sample. This experimental arrangement offers additional flexibility compared to one where the electron beam passes through the interior of the sample and minimizes possible damage of the sample by the electron beam, but it requires an analysis of the sensitivity of the experiment to the surface structure. The calculation of the probability of electron energy loss in this experimental setup has already been done for an ordered system of spheres located in a semiinfinite cubic lattice.[6,7] Here we deal with a system of random spherical inclusions, and our purpose is to analyze, in the same experimental arrangement, the effects of volume fraction, sizes, and spatial distribution of the inclusions. Our treatment uses the effective bulk dielectric response function.[3–5] The paper is organized as follows: In Sec. II we develop the formalism for the calculation of the energy loss in terms of a surface response function $g(Q,\omega)$ for longitudinal fields, and give an expression for $g(Q,\omega)$ in terms of a surface impedance. In Sec. III the surface impedance for three different models is calculated. The first two models correspond to local and nonlocal versions of a truncated bulk, where the surface impedance can be expressed in terms of the bulk dielectric function. The nonlocal version is known in the literature as the semiclassical infinite barrier (SCIB) model. This model is applied to the system of random spherical inclusions and results for the surface response function as well as the energy-loss probability are presented and discussed. The third model begins with the bulk nonlocal dielectric function, just as in the SCIB model, but the dielectric function is modified in such a way that the surface response function is consistent with a smooth surface profile. Finally, in Sec. IV we present our conclusions.

II. FORMALISM

Consider a half space filled with a system composed of a collection of identical spherical inclusions of radius a located at random and immersed in an otherwise homogeneous matrix; the other half space is vacuum. On the vacuum side, a high-energy electron travels on a classical rectilinear trajectory parallel to the interface at a nearly constant speed v_I. Our objective is to calculate the rate at which work is done on the electron by the induced electric field. Here we will neglect the effects of the magnetic field carried along by the traveling electron; this is known as the nonretarded approximation and it is valid to order $(v_I/c)^2$, where c is the speed of light.

Our first assumption is that if the system were unbounded, it could be described by an effective (or macroscopic), nonlocal, longitudinal dielectric function $\epsilon_l(k,\omega)$, derived by Barrera and Fuchs.[3] In this work it was assumed that the system appears homogeneous at a length scale $l \gg a$, although it is highly inhomogeneous at a length scale of the order of a.

The effective inverse nonlocal dielectric function is defined by

$$\frac{1}{\epsilon_l(\mathbf{k},\omega)} = 1 + \frac{\langle \phi^{\rm ind}(\mathbf{k},\omega)\rangle}{\phi^{\rm ext}(\mathbf{k},\omega)}; \tag{1}$$

this relates the average of the potential $\langle \phi^{\rm ind}\rangle$ induced in the system to the external potential $\phi^{\rm ext}$, where the average $\langle\cdots\rangle$ is taken over the macroscopic length scale. By *nonlocal* one means that $\epsilon_l(\mathbf{k},\omega)$ depends not only on the frequency ω of the exciting potential but also on its wave vector $\mathbf{k}$. For an unbounded, macroscopically homogeneous and isotropic system, the dielectric function depends on the magnitude k of the wave vector, not on its direction, and the stopping power of the electrons is directly related to Im $[1/\epsilon_l(k,\omega)]$.[8] It has been shown[3] that for the random system of spheres, $1/\epsilon_l(k,\omega)$ can be written in the following spectral representation:

$$\frac{1}{\epsilon_l(k,\omega)} = \frac{1}{\epsilon_2}\left[1 + f\left(\frac{C_b(k)}{u-1} + \sum_s \frac{C_s(k)}{u-n_s}\right)\right], \tag{2}$$

where $k=|\mathbf{k}|$ and

$$u = \frac{-1}{\epsilon_1/\epsilon_2 - 1} \tag{3}$$

is the spectral variable, which depends on ϵ_1 and ϵ_2, the local, frequency-dependent dielectric functions of the spheres and the matrix, respectively. The quantity $f=(N/V)4\pi a^3/3$ is the filling fraction of the spheres, where N is the total number of spheres, and V is the total volume of the system. By *spectral representation* we mean that $1/\epsilon_l(k,\omega)$ is written as a sum of terms with simple poles, and these poles are related to the excitation of the normal modes of the electric field within the system. In particular, the poles at $u=1$ and $u=n_s$ have strengths C_b and C_s, and correspond to the excitation of the bulk mode in medium 1 and interfacial modes, respectively.[9] Furthermore, the strengths C_b and C_s fulfill the sum rule

$$C_b + \sum_s C_s = 1, \tag{4}$$

which means that the sum of all mode strengths is conserved, or alternatively, that the strength of the bulk mode is reduced due to the presence of the interface, a fact also known as the *Begrenzung* effect.

Another appealing feature of the spectral representation given in Eq. (2) is that the properties of the material appear only in the spectral variable u, while the strengths of the poles depend on k and the geometry of the system. In the mean-field approximation the information about the geometry of the system is given by two statistical parameters:[3] the filling fraction f of spheres and their two-particle distribution function $\rho^{(2)}(R_{12})$, where R_{12} is the distance between the centers of two spheres. If $\rho^{(2)}(R_{12})$ takes account of only the excluded-volume correlation, that is, $\rho^{(2)}(R_{12})=1$ for $R_{12}\geqslant 2a$ and 0 otherwise, it can be shown[3] that the strengths of the modes C_b and C_s and the location of the interface modes n_s become functions of ka and are given by simple expressions, shown in detail in Appendix A. Here we need only note that

$$\lim_{ka\to\infty} C_b(ka) = 1 \tag{5a}$$

and

$$\lim_{ka\to\infty} C_s(ka) = 0. \tag{5b}$$

This means that in the limit of either large spheres or large wave vectors only the bulk mode will be excited.

Now we turn to the calculation of the energy loss of an electron traveling parallel to the planar interface of a semi-infinite system. First we define a coordinate system by taking the y axis at the interface and parallel to the electron trajectory and the z axis pointing towards the system. In this coordinate system the electron trajectory is given by $x=0$, $y=v_I t$, and $z=-z_0$, where z_0 is called the impact parameter. If we assume that the system has translational symmetry in the x and y directions, the probability per unit path length, per unit energy, of scattering with energy loss E, is given by (see Appendix B),

$$F(E) \equiv \frac{d^2P}{dl\ dE} = \frac{1}{a_0 E_I}\Xi(E), \tag{6}$$

where a_0 is the Bohr radius, E_I is the kinetic energy of the incident electron, and

$$\Xi(E) = \frac{1}{\pi}\int_0^\infty \frac{e^{-2Qz_0}}{Q}\ \text{Im}\ g(Q,\omega)\ dk_x, \tag{7}$$

with $E=\hbar\omega$ and $Q=\sqrt{k_x^2+\omega^2/v_I^2}$. The quantity $g(Q,\omega)$, known as the surface response function, is the complex reflection amplitude which relates the $(\mathbf{Q},\omega)$ Fourier components of the induced and external potentials:

$$\phi^{\rm ind}(\mathbf{Q},\omega) = -g(Q,\omega)\phi^{\rm ext}(\mathbf{Q},\omega). \tag{8}$$

Here, the Fourier component $\phi^{\rm ind}(\mathbf{Q},\omega)$ of the induced potential is related to $\phi^{\rm ind}(\boldsymbol{\rho},z;\omega)$ by a two-dimensional Fourier transform

$$\phi^{\rm ind}(\boldsymbol{\rho},z;\omega) = \int \frac{d^2Q}{(2\pi)^2}\ \phi^{\rm ind}(\mathbf{Q},\omega)\ e^{i\mathbf{Q}\cdot\boldsymbol{\rho}+Qz}; \quad -z_0 \leqslant z \leqslant 0, \tag{9}$$

where $\boldsymbol{\rho}=(x,y)$ is a two-dimensional vector parallel to the interface, and $\mathbf{Q}=(k_x,k_y)$ is a two-dimensional vector in k space. Similarly, the external potential $\phi^{\rm ext}(\mathbf{Q},\omega)$ is defined by

$$\phi^{\rm ext}(\boldsymbol{\rho},z;\omega) = \int \frac{d^2Q}{(2\pi)^2}\phi^{\rm ext}(\mathbf{Q},\omega)\ e^{i\mathbf{Q}\cdot\boldsymbol{\rho}-Qz}; \quad -z_0 \leqslant z \leqslant \infty. \tag{10}$$

The potentials $\phi^{\rm ind}(\boldsymbol{\rho},z;\omega)$ and $\phi^{\rm ext}(\boldsymbol{\rho},z;\omega)$ satisfy Laplace's equation in the regions indicated in Eqs. (9) and (10), since the charges that are sources of these potentials lie outside these regions. The difference of sign in $e^{\pm Qz}$ in these two equations arises because the induced and external charges are located in the regions $z\geqslant 0$ and $z\leqslant z_0$, respectively. Equation (7) is often written in terms of the surface loss function, defined as $S(Q,\omega)\equiv$ Im $g(Q,\omega)$.

In the following derivations we will take $\mathbf{Q}$ to lie in the x direction, which simplifies the notation and is permissable since we are assuming that the disordered system is invariant with respect to rotations about the z axis, so $g(Q,\omega)$ depends only on the magnitude of $\mathbf{Q}$, not its direction. By taking $E_x(\mathbf{Q},z,\omega)$ and $D_z(\mathbf{Q},z,\omega)$ as the two-dimensional Fourier transforms of $E_x(\boldsymbol{\rho},z,\omega)$ and $D_z(\boldsymbol{\rho},z,\omega)$ and demanding their continuity across the interface ($z=0$) one can express $g(Q,\omega)$ as

$$g(Q,\omega)=\frac{Z^V-Z(Q,\omega)}{Z^V+Z(Q,\omega)}, \tag{11}$$

where

$$Z(Q,\omega)\equiv i\,\frac{E_x(\mathbf{Q},\ z=0^+,\omega)}{D_z(\mathbf{Q},\ z=0^+,\omega)} \tag{12}$$

plays the role of a surface impedance of the medium and $Z^V=1$ is the corresponding surface impedance of vacuum. It is not surprising that the expression for $g(Q,\omega)$ in Eq. (11) has the characteristic form of a reflection amplitude because one can think of $\phi^{\rm ext}(\boldsymbol{\rho},z;\omega)$ and $\phi^{\rm ind}(\boldsymbol{\rho},z;\omega)$ in the region $-z_0\leqslant z\leqslant 0$, as ''incident'' and ''reflected'' potentials, respectively.

III. MODELS

In general, the calculation of Z would require a precise model for the bulk and surface region of the system together with the complete solution for the fields. Nevertheless, there are two simple models in which it is possible to obtain an expression for Z in terms of the bulk dielectric response functions of the system. These are the local limit and the semiclassical infinite barrier model (SCIB). Both models possess a sharp boundary at the surface and they can be regarded as local and nonlocal variants of a truncated bulk. Here we will apply them to the system of random spherical inclusions described above in order to analyze their results and significance. We will also use a modified SCIB model which takes account of the actual sphere density profile near the surface more accurately.

A. Local limit

In the local limit one assumes that the bulk longitudinal dielectric response of the system $\epsilon_B(k,\omega)$ is independent of k; i.e., one replaces $\epsilon_B(k,\omega)$ by $\epsilon_B(\omega)=\epsilon_B(k=0,\omega)$, for $z\geqslant 0$. In this case the surface impedance is

$$Z_{\rm loc}(\omega)=\frac{1}{\epsilon_B}, \tag{13}$$

and the substitution of Eq. (13) into Eq. (11) yields

$$g(\omega)=\frac{1-1/\epsilon_B}{1+1/\epsilon_B}=\frac{\epsilon_B-1}{\epsilon_B+1}. \tag{14}$$

Now, substituting $g(\omega)$ into Eq. (7) and performing the integration over k_x, one gets the well-known local result[10]

$$F(E)=\frac{1}{a_0E_I}\,\Xi_{\rm loc}(E), \tag{15}$$

where

$$\Xi_{\rm loc}(E)=\frac{1}{\pi}K_0\left(\frac{2z_0}{v_I/\omega}\right)\ {\rm Im}\left[\frac{\epsilon_B(\omega)-1}{\epsilon_B(\omega)+1}\right], \tag{16}$$

with K_0 the modified Bessel function of order zero. The argument of K_0 establishes the characteristic length v_I/ω which determines approximately the maximum value of impact parameter for which the probablility of energy loss is appreciable. For the system of random spherical inclusions,

$$\frac{1}{\epsilon_B(\omega)}=\frac{1}{\epsilon_l(k=0,\omega)}=\frac{1}{\epsilon_2}\left[1+f\frac{1}{u-n_1}\right], \tag{17}$$

with $n_1=(1+2f)/3$. Equation (17) corresponds to the Maxwell-Garnett bulk dielectric function which takes account only of the dipolar modes excited in each sphere, and whose shortcomings were already discussed in Ref. 3. These dipolar modes are driven by surface charges induced at the interface of each sphere and their coupling gives rise to a collective dipolar mode known as the dipole interface plasmon. The location of this mode corresponds to the pole in Eq. (17) located at $u=n_1=(1+2f)/3$.

Applying this model to a concrete example, we have calculated the energy-loss probability function $\Xi_{\rm loc}(E)$ for a half space of aluminum spheres in vacuum. In this case, $\epsilon_2=1$ and $\epsilon_1(\omega)$ is given by a Drude dielectric function

$$\epsilon_1(\omega)=1-\frac{\omega_p^2}{\omega(\omega+i/\tau)}, \tag{18}$$

where ω_p is the bulk plasma frequency and τ, the relaxation time coming from dissipation processes, is considered as a parameter which controls the width of the excitation peaks. For aluminum $\hbar\omega_p=16.0$ eV, and we take $\omega_p\tau=100$. The dotted line in Fig. 1 shows the results of this local calculation for two different values of the filling fraction, $f=0.15$ and 0.5, and two values of the impact parameter, $z_0=1$ and 10 Å. In all cases the energy-loss spectrum is a single sharp peak which is shown reduced in height by the factor N given in the ($\times N$) legend, in order to fit the results of subsequent calculations on the same plot.

This peak arises from the dipole interface-plasmon excitations of the system of aluminum spheres in vacuum. A simple expression for the position of this peak can be found by setting $\tau=\infty$ in Eq. (18). One can see from Eq. (16) that in the half space the resonance frequency of the dipolar mode, which we denote by ω_s, is determined by the condition $\epsilon_B(\omega)=-1$. From Eq. (17) the corresponding pole in the spectral variable u is $n_s=(1+f/2)/3$ and the resonance frequency is $\omega_s=\omega_p\sqrt{n_s}=\omega_p\sqrt{(1+f/2)/3}$. These results show that the dipolar mode frequency ω_s increases from $\omega_p/\sqrt{3}$ to $\omega_p/\sqrt{2}$ as f increases from 0 to 1. One readily finds that the energy of the dipolar excitation for the half space is $\hbar\omega_s=9.6$ eV for $f=0.15$ and $\hbar\omega_s=10.3$ eV for $f=0.5$, values which agree with the positions of the local peaks in Fig. 1. The single peak in $\Xi_{\rm loc}(E)$ is relatively narrow, since the width of the peak comes solely from the dissipation process included in the Drude dielectric response

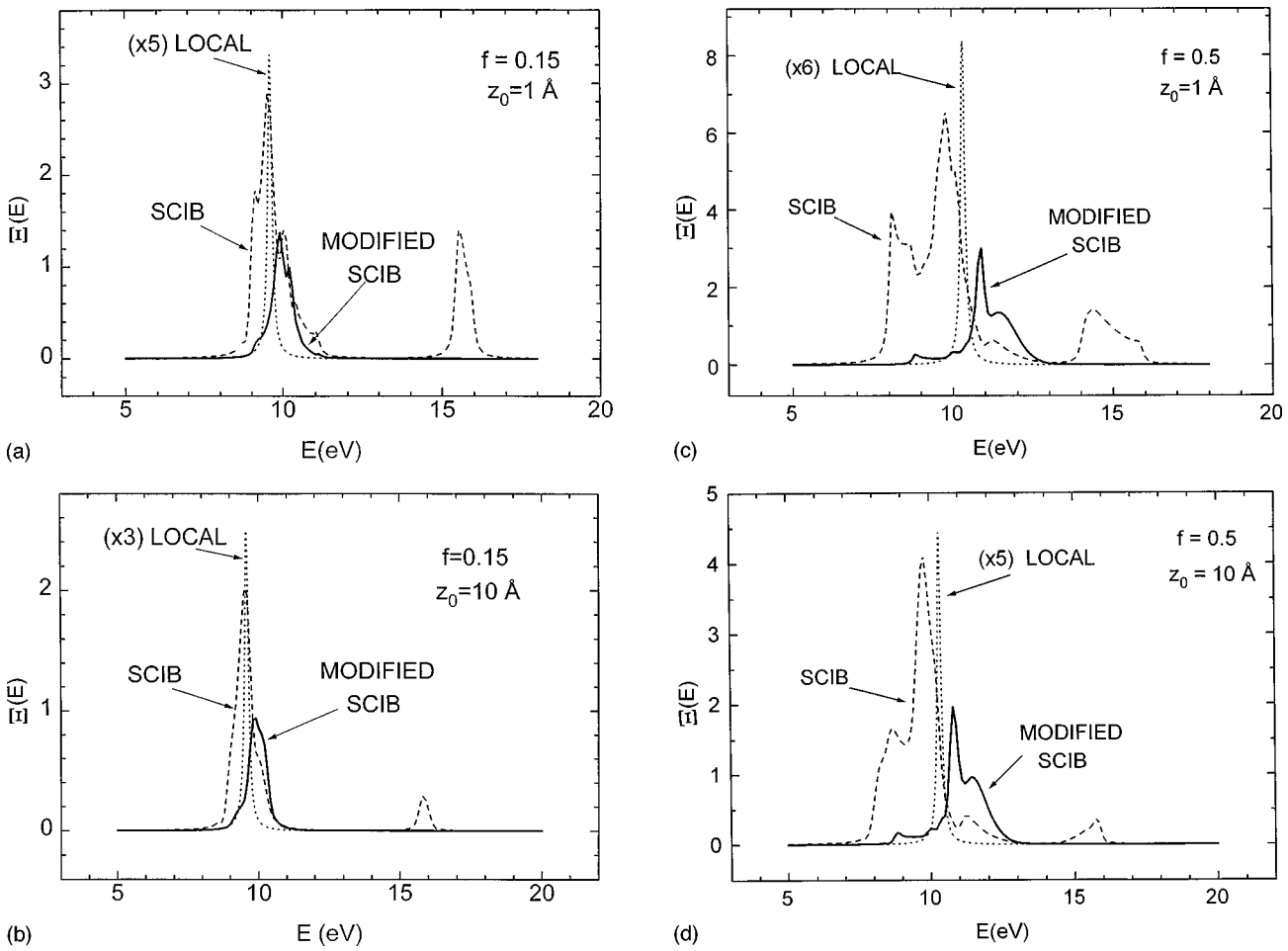

FIG. 1. (a) Energy-loss probability function $\Xi(E)$ as a function of the energy loss E, for a filling fraction $f=0.15$ and an impact parameter $z_0=1$ Å. The dotted line corresponds to the local model, the dashed line to the SCIB model, and the solid line to the modified SCIB model. The notation $(\times N)$ attached to a curve in these figures indicates that the values shown on the ordinate axis for that curve must be multiplied by the factor N. (b) The same as in (a) but for $z_0=10$ Å. (c) The same as in (a) but for $f=0.5$. (d) The same as in (c) but for $z_0=10$ Å.

$\epsilon_1(\omega)$ of the spheres through the parameter $1/\tau$. It is also evident that the sphere radius does not enter into this local model.

B. Semiclassical infinite barrier (SCIB) model

1. Description of the model

The SCIB model has traditionally been applied to describe the response of a semi-infinite electron gas.[11] In this model one is able to calculate the surface impedance Z in terms of a known bulk nonlocal dielectric response $\epsilon_B(k,\omega)$. The idea is to replace the system in a half space by an unbounded system described by $\epsilon_B(k,\omega)$. Then one looks for solutions of Maxwell's equations for the electric and displacement fields with specular symmetry about the interface plane, i.e., $E_x(x,y,z,\omega)=E_x(x,y,-z,\omega)$ and $E_z(x,y,z,\omega)=-E_z(x,y,-z,\omega)$, with similar equations for D_x and D_z. One assumes that the fields with physical reality are those on only one side of the interface, the side where the actual system is located, and then one matches these fields with the actual fields in the vacuum using the continuity of E_x, E_y, and D_z. This procedure tacitly assumes a model for the interface, which in the case of an electron gas can be interpreted as if the surface were acting as an infinite potential barrier causing the specular reflection of the electrons, but neglecting the quantum interference terms; this is the origin of the term *semiclassical infinite barrier* and also of the term *specular reflection model* which is often used. This procedure yields[11,8]

$$Z(Q,\omega)=\frac{Q}{\pi}\int_{-\infty}^{+\infty}\frac{dk_z}{(Q^2+k_z^2)\epsilon_B(k,\omega)}. \tag{19}$$

Here we apply this model to the system of random spherical inclusions by using $\epsilon_l(k,\omega)$ given in Eq. (2) as the bulk nonlocal dielectric response function $\epsilon_B(k,\omega)$. In Eq. (19), the magnitude of the wave vector is $k=\sqrt{Q^2+k_z^2}$. The electron-energy-loss function $\Xi(E)$ is then readily obtained by using Eqs. (11) and (7).

Before presenting the results of this model we will analyze the behavior of the fields and the polarization charges in the neighborhood of the interface. The boundary conditions of the fields at the interface demand the continuity of E_x, E_y, and D_z, and it can be shown[12,13] that

$$E_z(\mathbf{Q},z=0^-,\omega)=\epsilon_\infty(\omega)\,E_z(\mathbf{Q},z=0^+,\omega), \tag{20}$$

where $E_z(\mathbf{Q},z,\omega)$ is the two-dimensional Fourier transform of the electric field $E_z(x,y,z,\omega)$ with respect to x and y, and

$$\epsilon_\infty(\omega)=\lim_{k\to\infty}\epsilon_l(k,\omega), \tag{21}$$

is known as the background dielectric function of the system. In the usual model of a metal, one can write the total dielectric function as the sum of a contribution from the conduction electrons, which goes to zero as $k\to\infty$, and a k-independent contribution from core electrons. Therefore, the core electrons are the source of a local background dielectric function $\epsilon_\infty>1$.

In our system of random spherical particles, the origin of the background dielectric function is quite different. By combining Eqs. (2), (3), and (5a), and (5b), we have

$$\frac{1}{\epsilon_\infty(\omega)}=\frac{f}{\epsilon_1}+\frac{1-f}{\epsilon_2}. \tag{22}$$

In the absence of the spheres, that is, in the limit $f\to 0$, one gets $\epsilon_\infty=\epsilon_2$, which is what is expected, since ϵ_2 plays the role of a local background for the system of polarizable spheres. When spheres are present ($f>0$), a term f/ϵ_1 appears in Eq. (22). This term arises from the bulk mode strength $C_b(k\to\infty)=1$ in Eq. (2) and it corresponds to a bulk plasmon resonance of the spheres. One can also show that when there is a background dielectric function $\epsilon_\infty\neq 1$, a surface charge density $\sigma^{\rm ind}(\mathbf{Q},\omega)$ at $z=0$ appears:

$$\sigma^{\rm ind}(\mathbf{Q},\omega)=-\frac{[\epsilon_\infty(\omega)-1]}{4\pi}E_z(\mathbf{Q},z=0^+,\omega). \tag{23}$$

In addition to this surface charge, there is also a volume distribution of charge due to the nonlocal nature of $\epsilon_l(k,\omega)$ for finite k.

2. Results and discussion

Here we present results for the system of random spherical inclusions within the SCIB model. The bulk dielectric response $\epsilon_l(k,\omega)$ is taken in the mean-field approximation and we consider only the excluded-volume correlation between spheres. In this case C_b, C_s, and n_s are functions of ka and are calculated using the expressions given in Eqs. (A1)–(A4). The calculation is performed by truncating the multipolar sums to a maximum value $L=6$. Therefore the locations n_s and the strengths C_s of the first six interfacial modes are obtained by finding the eigenvalues and eigenvectors of the 6×6 matrix $H_{ll'}$ given by Eq. (A4). The rest of the modes (with $s>6$) are taken into account by including an additional ''effective'' mode whose location $n_{\rm eff}$ and strength $C_{\rm eff}$ are determined by sum rules, as shown in detail in Appendix C.

We again present results for a half space of aluminum spheres in vacuum, using the same Drude dielectric function $\epsilon_1(\omega)$ for aluminum, Eq. (18), as for the local model. In addition to the bulk plasmon energy of 16.0 eV for the aluminum, there are two other important characteristic energies: the surface plasmon energy for a half space filled with aluminum, $\hbar\omega_{\rm sp}=\hbar\omega_p/\sqrt{2}=11.3$ eV, and the energy of the dipolar mode of an isolated sphere, $\hbar\omega_d=\hbar\omega_p/\sqrt{3}=9.2$ eV.

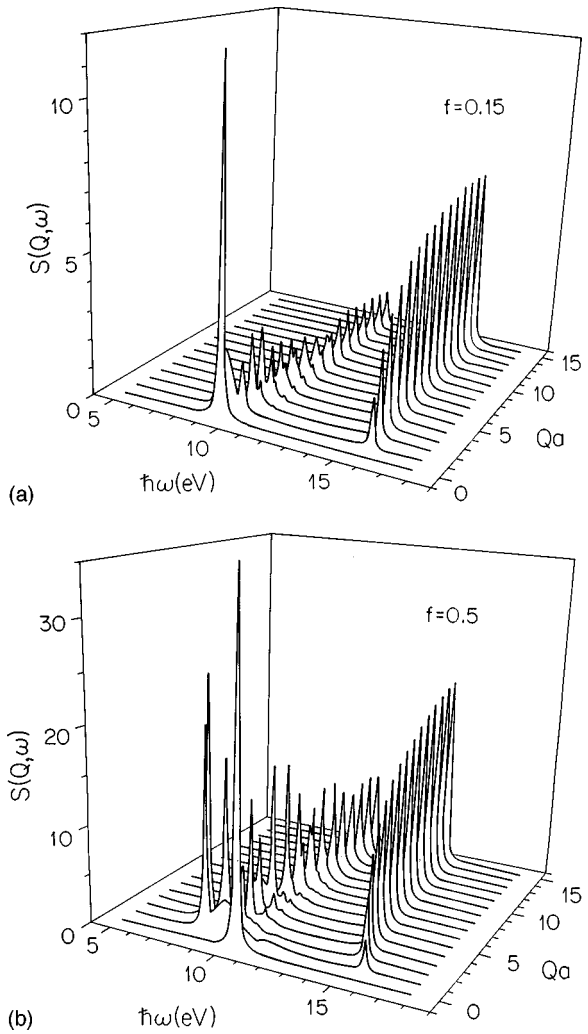

FIG. 2. (a) Surface loss function $S(\mathbf{Q},\omega)$, as a function of Qa and $\hbar\omega$, for aluminum spheres in vacuum using the SCIB model and a filling fraction $f=0.15$. (b) The same as in (a) but for $f=0.5$.

In Fig. 2 we show a plot of $S(Q,\omega)\equiv$ Im $g(Q,\omega)$ as a function of Qa and $\hbar\omega$ for $f=0.15$ and 0.5, and $\omega_p\tau=100$. For $Qa=0$ there is a single peak around 9.6 eV for $f=0.15$ and around 10.3 eV for $f=0.5$. Then, as Qa increases, two things happen: (i) a single, isolated peak at about 16 eV starts to emerge, increasing in height and shifting slightly towards lower energies, this shift being more pronounced for $f=0.5$ than for $f=0.15$, and (ii) a multipeaked structure appears in the low-energy region: between 8.5 and 11.0 eV for $f=0.15$, and between 7.0 and 12.0 eV for $f=0.5$. For both values of f, this structure becomes a single peak when $Qa>10$; this occurs because we have replaced the high-multipolar interfacial modes by a single ''effective'' mode. Nevertheless, since the actual multipolar structure becomes narrower as Qa increases, the effective-mode approximation is adequate.

What is the physical origin of these peaks? One can identify the low-energy peaks with the usual surface modes coming from the term $\Sigma C_s/(u-n_s)$ in Eq. (2), while the high-energy peak comes from the term $C_b/(u-1)$ in Eq. (2). First consider the $Q\to 0$ limit. In this limit the factor $1/(Q^2+k_z^2)$ in Eq. (19) is very sharply peaked at $k_z=0$, so

only the local limit $\epsilon_l(k=0,\omega)$ contributes. Equation (19) gives $Z=1/\epsilon_l(\omega)$, where $\epsilon_l(\omega)\equiv\epsilon_l(k=0,\omega)=1-f/[u-(1-f)/3]$ is the Maxwell-Garnett dielectric response.[3] According to Eq. (11) there is a pole in $g(0,\omega)$, and a corresponding peak in $S(Q=0,\omega)\equiv$ Im $g(0,\omega)$ when $Z=-1$ or $\epsilon_l(\omega_s)=-1$. For an electron gas this condition yields $\omega_s=\omega_d\sqrt{1+f/2}$, where $\omega_d=\omega_p/\sqrt{3}$ is the dipolar resonance of an isolated sphere. For aluminum $\hbar\omega_p=16.0$ eV, and so, $\hbar\omega_s=9.6$ eV for $f=0.15$, while for $f=0.5$, one has $\hbar\omega_s=10.3$ eV. Thus, in Fig. 2, the only peak observed in $S(Q=0,\omega)$ can be identified with the surface mode of a flat interface described by the corresponding Maxwell-Garnett local dielectric function, and this peak has the same location as the peak in the energy-loss function obtained using the local model. The shift in position and decrease in height of this peak as Q increases is due to the nonlocal nature of the actual dielectric response.

The other peak which appears at finite Q close to the bulk plasmon energy is due to the presence of the aluminum dielectric function $\epsilon_1(\omega)$ in the background $\epsilon_\infty(\omega)$. The position of this peak can be understood by first looking at the $Q\to\infty$ limit. Since $k^2=Q^2+k_z^2$ this limit is equivalent to $k\to\infty$, so the nonlocal dielectric function $\epsilon_l(k,\omega)$ in Eq. (19) can be replaced by the background dielectric function $\epsilon_\infty(\omega)$. Equation (19) then gives $Z=1/\epsilon_\infty(\omega)$. Therefore, a peak in $S(Q=\infty,\omega)$ will appear at an energy $\hbar\omega_H$ such that $\epsilon_\infty(\omega_H)=-1$. Now, setting $\epsilon_2=1$ in Eq. (22) and inserting for ϵ_1 the Drude response of Eq. (18) with $\tau\to\infty$, one gets $\hbar\omega_H=\hbar\omega_p\sqrt{1-f/2}$, which starts from the bulk plasma frequency at $f=0$ and shifts to lower energies as f increases, attaining the surface plasmon value $\hbar\omega_s=\hbar\omega_p/\sqrt{2}$ for $f=1$. For aluminum, one gets $\hbar\omega_H=15.4$ eV for $f=0.15$ and $\hbar\omega_H=13.9$ eV for $f=0.5$. We identify this peak with the high-energy peak which appears in $S(Q,\omega)$ in Fig. 2, in the limit $Qa\to\infty$. This also explains why the redshift of this peak is larger for $f=0.5$ than for $f=0.15$. In conclusion, $S(Q,\omega)$ has a two-peak structure for any finite Q, but it has a single-peak structure in two limiting cases: $Q\to0$ and $Q\to\infty$. The small-Q limit corresponds to the excitation by a constant field and can be identified with the Maxwell-Garnett local approximation, and the large-Q limit corresponds to the excitation of the background.

We now substitute the results for $S(Q,\omega)$, shown in Fig. 2, into Eq. (7) and perform the k_x integration to get $\Xi(E)$. In Fig. 1 we plot $\Xi(E)$ as a function of E for two values of the impact parameter, $z_0=1$ and 10 Å, and two different values of the filling fraction, $f=0.15$ and 0.5. The sphere radius is taken as $a=25$ Å. In contrast with the single peak in $\Xi_{\rm loc}(E)$ found in the local model, the SCIB model gives a broad and rich multipeaked structure in $\Xi(E)$. There is structure in a low-energy region, from about 8 to 12 eV for $f=0.15$ and from 6 to 13 eV for $f=0.5$, and also in a high-energy region below 16 eV. The width of this structure comes from both the nonlocal nature of the effective bulk response $1/\epsilon_l(k,\omega)$ and the dissipation process included in the Drude response $\epsilon_1(\omega)$. In other words, the profile of $\Xi(E)$ is closely related to the low-energy structure and the high-energy peaks of $S(Q,\omega)$. For both filling fractions the strengths of the peaks in the low-energy region are greater than the strengths of high-energy peaks. Although the strength in both regions decreases as z_0 increases, it is also clear that the strength of the high-energy peaks decreases faster. For example, for $z_0=10$ Å, the strength of the high-energy peak is already very small in comparison with that of the tallest peak in the low-energy region. Also, the structure in both energy regions becomes narrower as the filling fraction decreases. For example, for $z_0=10$ Å and $f=0.15$ the low-energy structure becomes almost a single peak with small shoulders on both the low- and high-energy sides.

C. Modified SCIB model

In this section we shall present evidence that the high-energy peak which appears in $S(Q,\omega)$ and in the energy-loss spectrum should not appear when the electron trajectory is outside the material and discuss why the abrupt termination of the surface at $z=0$ in the standard SCIB model gives this high-energy peak. To remedy these shortcomings, we shall use qualitative arguments to construct a modified SCIB model that is consistent with the actual smooth sphere density profile near the surface, and for which the high-energy peak is absent.

1. Abrupt termination of the surface in the SCIB model

We first discuss why the SCIB model corresponds to an abrupt termination of the surface at $z=0$. One expects this to be true from the qualitative argument that the SCIB model uses the bulk dielectric function $\epsilon_l(k,\omega)$ of an unbounded random system of spheres, so the distribution of spheres is the same near the surface as it is deep within the system. That is, the volume fraction of spheres has a constant value f everywhere in the half space $z>0$. This also can be shown quantitively in the following way.

Consider a two-component system with arbitrary geometry, confined to the half space $z>0$, which has translational symmetry in the x and y directions after configurational averaging. Let the local dielectric functions of the two components be $\epsilon_1(\omega)$ and $\epsilon_2=1$, respectively, so the spectral variable is $u=-1/(\epsilon_1-1)$. It has been shown[5] that the surface response function $g(Q,\omega)$ has a spectral representation

$$g(Q,\omega)=-\frac{f}{2}\int_0^1\frac{D(Q,n)\,dn}{u-n},\tag{24}$$

where f is the volume fraction of component 1 infinitely far from the surface, where it is presumed to have a constant value. The spectral function $D(Q,n)$ is real and positive, with a nonzero value only in the region $0\leqslant n\leqslant1$. In Ref. 5 the following sum rule for the zeroth moment $\mu_0(Q)$ of the spectral function is derived:

$$\mu_0(Q)\equiv\int_0^1 D(Q,n)\,dn=\frac{2Q}{f}\int_0^\infty e^{-2Qz}f(z)\,dz.\tag{25}$$

Here $f(z)$, the z-dependent volume fraction of component 1, is the fraction of a plane surface at a given value of z that is within component 1. The ''normalizing constant'' $f/2$ in Eq. (24) has been chosen so that $\mu_0(Q)=1$ for a half space with a constant volume fraction of component 1, $f(z)=f$ for $z\geqslant0$.

Now, it can be shown that the spectral function corresponding to the SCIB model for the surface response function has zeroth moment $\mu_0=1$. The proof involves expanding the surface response function in increasing powers of $1/u$ and comparing the u^{-1} terms. From Eqs. (24) and (25) we find $g=-\frac{1}{2}f\ \mu_0\ u^{-1}+O(u^{-2})$. On the other hand, Eqs. (2) and (4) give $1/\epsilon_l=1+f\ u^{-1}+O(u^{-2})$. The integral in Eq. (19) can be done immediately, so $Z=1+f\ u^{-1}+O(u^{-2})$, and Eq. (11) gives $g=-\frac{1}{2}f\ u^{-1}+O(u^{-2})$. Comparing the u^{-1} terms in these two expressions for g gives the desired result, $\mu_0=1$. Therefore the SCIB model is consistent with a constant volume fraction of spheres $f(z)=f$ in the half space $z>0$.

Following the derivation in the preceding paragraph, but using Eq. (2) before applying the sum rule in Eq. (4), one can show that the zeroth moment is the sum of separate contributions from the bulk mode and the surface modes:

$$\mu_0=\mu_0^{(B)}(Q)+\mu_0^{(S)}(Q)=1, \tag{26}$$

where

$$\mu_0^{(B)}(Q)=\frac{2Q}{\pi}\int_0^\infty C_b(k)\frac{dk_z}{Q^2+k_z^2}, \tag{27}$$

$$\mu_0^{(S)}(Q)=\frac{2Q}{\pi}\int_0^\infty \sum_s\ C_s(k)\frac{dk_z}{Q^2+k_z^2}, \tag{28}$$

with $k^2=Q^2+k_z^2$. These equations will be used later for constructing the modified SCIB model.

We now present some arguments which suggest that the high-energy peak in Figs. 1 and 2, which comes from the bulk mode term $C_b/(u-1)$ in Eq. (1), is an artifact of the SCIB model and should not appear when the fast electrons travel on a trajectory outside the surface. First, it is well known that an electron traveling on a classical rectilinear trajectory can excite a bulk plasmon on a sphere described by a local dielectric function, only in the case this trajectory crosses the sphere.[10,14] Since in our case the trajectory of the electron does not cross any of the spheres, one would expect a coupling only to the interfacial modes. Second, in the derivation of the equation for $\epsilon_l(k,\omega)$, which is used to calculate the energy loss of electrons passing through the random system of spheres, an external charge density of the form $\rho(z)=\rho_0\ e^{ikz}$ was applied.[3] This work showed that the bulk mode term arises entirely from the part of the external charge density inside the spheres. Since this external charge density represents the overlap of initial and final wave functions for electrons scattered by the system, one would expect that if the electrons did not enter the spheres, the external charge density inside the spheres would be zero, and that there would be no bulk mode excitation.

In the SCIB model, the external charge in the fictitious infinite medium is a surface charge density on the $z=0$ plane associated with the discontinuity of D_z: $4\pi\sigma^{\rm ext}=2D_z(z=0+)$. Clearly this external charge is inside those spheres which are cut by the $z=0$ plane. Indeed, in the limit $Q\to\infty$ (or $k\to\infty$), the potential due to this charge becomes localized at the $z=0$ plane, so no interfacial modes are excited. Also, in this limit the inverse dielectric function given by Eq. (22) simply represents the screening of the external charge by the dielectric functions of the two media, weighted by the factors f and $1-f$, which are the probabilities that the external charge lies inside media 1 and 2, respectively.

2. Smooth surface profile

In this section we derive expressions for the z-dependent volume fraction of spheres, $f(z)$. We shall show that for any physically reasonable distribution of spheres, $f(z)$ must be a continuous function of z, and in particular, $f(z)$ cannot change discontinuously from a constant value f for $z>0$ to the value zero for $z<0$, as in the standard SCIB model. We shall also find a specific result for $f(z)$, assuming a very simple distribution of sphere positions, and use this result to calculate the zeroth moment of the half-space spectral function.

Assume that all spheres have the same radius, a. For an infinite three-dimensional system that is translationally invariant after suitable configurational averaging, the relation between the (constant) volume fraction f of spheres and the density n of sphere centers is $f=4/3\ \pi a^3 n$. However, if the spheres are confined to a half space, both the density of sphere centers and the volume fraction of spheres depend on z.

To find the relation between $f(z)$ and $n(z)$, first take a single sphere with center at z_i, and imagine that the sphere is cut by a plane of area L^2 at a given value of z. The contribution of the sphere to the volume fraction at this value of z, which we denote $f_i(z)$, is the fraction of the area L^2 that is contained within the sphere,

$$f_i(z)=\pi[a^2-(z-z_i)^2]/L^2, \tag{29}$$

for $z_i-a\leqslant z\leqslant z_i+a$. If $|z-z_i|>a$, the plane does not intersect the sphere, so $f_i(z)=0$. The total contribution of all spheres to $f(z)$ is found by replacing z_i in Eq. (29) by a continuous variable z', multiplying by $L^2 n(z')\,dz'$ where $n(z')$ is the density of sphere centers, and integrating over z':

$$f(z)=\pi\int_{z-a}^{z+a} n(z')[a^2-(z-z')^2]\,dz'. \tag{30}$$

If the spheres cannot penetrate the surface plane $z=0$, the sphere centers must lie in the region $z\geqslant a$, so $n(z)=0$ for $z<a$. In the region $z>a$, $n(z)$ depends on the density of spheres and their positions in the half space. We can find a specific expression for $f(z)$ by making the simplest possible assumption for $n(z)$ in the region $z\geqslant a$, i.e., $n(z)=n=$ const. With this assumption, Eq. (30) yields

$$\begin{aligned} f(z)&=\frac{3}{4}\left[\left(\frac{z}{a}\right)^2-\frac{1}{3}\left(\frac{z}{a}\right)^3\right]f, \quad 0<z<2a \\ &=f, \quad z>2a. \end{aligned} \tag{31}$$

Figure 3 shows the step function $n(z)$ and the associated continuous function $f(z)$.

The zeroth moment of the spectral function $D(n)$, defined by Eq. (24), must have a value given by the sum rule (25). If we use the density profile $f(z)$ given by Eq. (31) in Eq. (25) to calculate the zeroth moment, which we denote by $\mu_0^{(M)}(Q)$, the result is

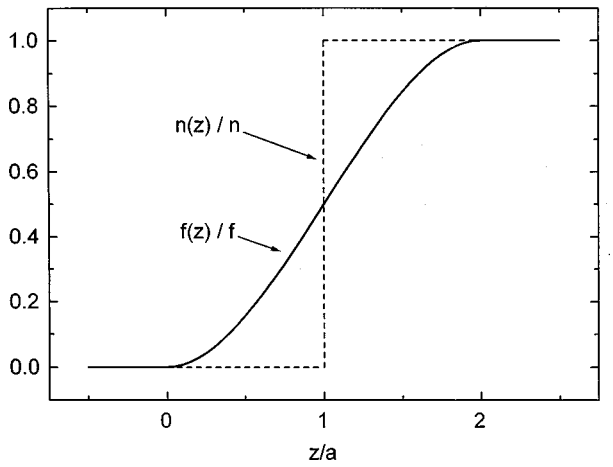

FIG. 3. The z-dependent volume fraction of spheres $f(z)$ as a function of z/a, when the density $n(z)$ of sphere centers is taken as a step function. The dashed line is the step function $n(z)/n$ and the solid line is the corresponding $f(z)/f$.

$$\mu_0^{(M)}(Q)=e^{-4Qa}+\frac{3}{2}Qa\ \lambda(2Qa), \tag{32}$$

where

$$\lambda(x)=2\left[\frac{1}{x^3}-\frac{1}{x^4}-e^{-2x}\left(\frac{2}{3x}-\frac{1}{x^3}-\frac{1}{x^4}\right)\right]. \tag{33}$$

Figure 4 shows a plot of $\mu_0^{(M)}(Q)$ as a function of Qa. Recall that $\mu_0=1$ for a constant volume fraction in the half space $f(z)=f$ for $z\geq 0$. The result $\lim_{Q\to 0}[\mu_0^{(M)}(Q)]=1$ can be understood from the fact that the external potential penetrates infinitely deeply into the half space in the small-Q limit, so the falloff of $f(z)$ within a distance $2a$ from the surface has no effect, and only the (constant) value $f(z)=f$ far from the surface is important. The external potential penetrates less deeply into the half space as Qa increases, so the continuously decreasing $f(z)$ near the surface causes a corresponding decrease of $\mu_0^{(M)}(Q)$.

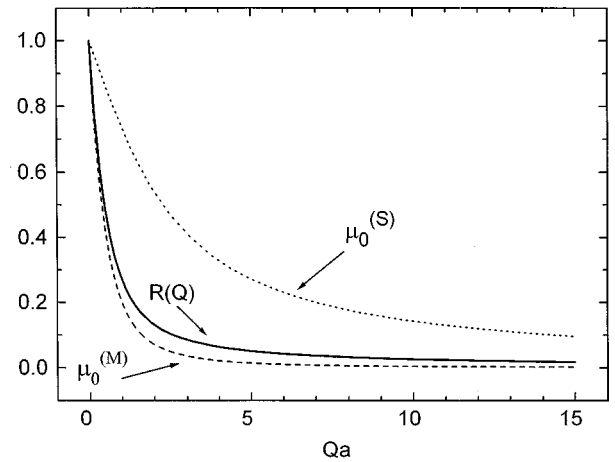

FIG. 4. The dotted line is the interface-mode contribution $\mu_0^{(S)}$ to the zeroth moment μ_0 of the spectral function $D(Q,n)$, as a function of Qa, for the SCIB model. The dashed line is the zeroth moment $\mu_0^{(M)}$ of the spectral function $D(Q,n)$, as a function of Qa, when the z-dependent volume fraction of spheres $f(z)$, shown in Fig. 3, is used in the sum rule given by Eq. (25). The solid line corresponds to the ratio $R(Q)=\mu_0^{(M)}(Q)/\ \mu_0^{(S)}(Q)$, as a function of Qa.

3. Description of modified SCIB model

The standard SCIB model applied to a system of random spherical particles in a half space has two defects. First, we have presented arguments which suggest that the high-energy loss peak, which arises from the bulk mode term $C_b/(u-1)$ in Eq. (2), should not be present. Second, the model does not take account of the continuous surface profile $f(z)$ correctly since it gives a constant value for zeroth moment, $\mu_0=1$, which does not agree with the decreasing zeroth moment $\mu_0^{(M)}(Q)$ shown in Fig. 4.

In order to correct these defects, we propose the following modified SCIB model. First, we simply omit the bulk mode term in Eq. (2) by setting $C_b=0$. Second, we modify the remaining surface mode terms so that the zeroth moment of the spectral function agrees with the ''exact'' value $\mu_0^{(M)}(Q)$ found from our simple model of a smooth surface profile. In order to make this modification, we note that the surface mode terms in Eq. (2) give a value of $\mu_0^{(S)}(Q)$ that can be calculated from Eq. (28). If we use an approximate analytic form for the total strength of the surface modes,[4]

$$\sum_s C_s(k)\simeq\frac{b}{\sqrt{\rho^2+b^2}}, \tag{34}$$

where $\rho=ka$ and $b=2.262$, Eq. (28) gives

$$\mu_0^{(S)}(Q)=\frac{2}{\pi}\arctan\left(\frac{b}{Qa}\right). \tag{35}$$

A plot of $\mu_0^{(S)}(Q)$ as a function of Qa is shown in Fig. 4. Clearly $\mu_0^{(S)}(Q)>\mu_0^{(M)}(Q)$, so the zeroth moment is still too large, even after removing the bulk mode. The most straightforward way to get the correct zeroth moment $\mu_0^{(M)}(Q)$ is to multiply all surface mode strengths by the ratio

$$R(Q)=\frac{\mu_0^{(M)}(Q)}{\mu_0^{(S)}(Q)}. \tag{36}$$

The ratio $R(Q)$ is plotted as a function of Qa in Fig. 4.

Therefore, the modified SCIB model consists of replacing the inverse bulk dielectric function $1/\epsilon_l(k,\omega)$ in Eq. (19) by a modified inverse dielectric function

$$\frac{1}{\epsilon_l^{(M)}(\mathbf{k},\omega)}=\frac{1}{\epsilon_2}\left[1+f\ R(Q)\ \sum_s\frac{C_s(k)}{u-n_s(k)}\right]. \tag{37}$$

Since $R(Q)$ falls off rapidly as Q increases, the dispersion of the interfacial modes at large values of k will play a smaller role in the modified SCIB model than in the original SCIB model. Therefore, the modified SCIB model should give a narrower energy-loss spectrum, closer to the spectrum of the local model. These qualitative expectations will be borne out by the numerical calculations discussed in the following section.

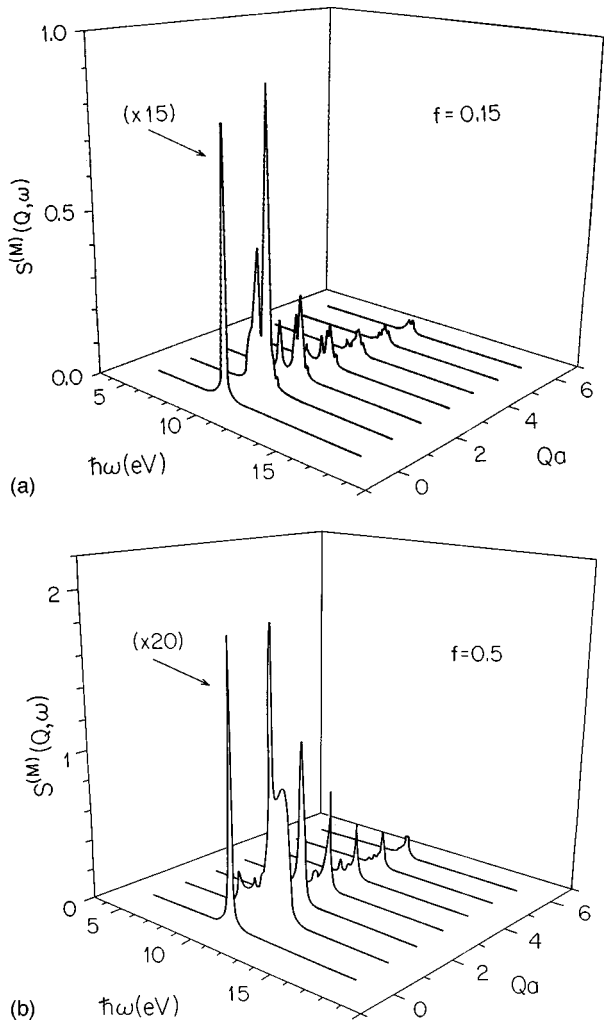

FIG. 5. (a) Surface loss function $S^{(M)}(\mathbf{Q},\omega)$, as a function of Qa and $\hbar\omega$, for aluminum spheres in vacuum using the modified SCIB model and a filling fraction $f=0.15$. (b) The same as in (a) but for $f=0.5$.

4. Results and discussion

By substituting $1/\epsilon_l^{(M)}(\mathbf{k},\omega)$ into Eq. (19) for the surface impedance and using Eq. (11) one obtains an expression for the surface loss function $S^{(M)}(Q,\omega)\equiv$ Im $g^{(M)}(Q,\omega)$ corresponding to the modified SCIB model. In Fig. 5 we show $S^{(M)}(Q,\omega)$ as a function of Qa and $\hbar\omega$ for $f=0.15$ and 0.5. Obviously, since the bulk plasma mode has been removed from the bulk dielectric response $1/\epsilon_l$, there is no structure in $S^{(M)}(Q,\omega)$ around $\hbar\omega\approx 15$ eV. For $Qa=0$ there is a single isolated peak which is the same as in the standard SCIB model. Then for $Qa>0$ a multipeaked structure appears which is considerably reduced in strength when compared with the structure in the low-energy region of $S(Q,\omega)$ in the standard SCIB model, as shown in Fig. 2. Also, as Qa increases there is an extremely fast overall decrease of $S^{(M)}(Q,\omega)$. For example, for both filling fractions, $f=0.15$ and $f=0.5$, and $Qa=6$, $S^{(M)}(Q,\omega)$ has almost vanished. This behavior comes, obviously, from the fast drop of $R(Q)$, as a function of Qa, as can be seen in Fig. 4.

We now calculate $\Xi(E)$ for the modified SCIB model by substituting $S^{(M)}(Q,\omega)$ into Eq. (7). The results are shown in Fig. 1, together with the results of the other two models mentioned above, for the same two filling fractions and impact parameters, that is, $f=0.15$ and 0.5 , and $z_0=1$ and 10 Å. One can see that $\Xi(E)$ now has a weak dependence on z_0, that the isolated structure below 16 eV has disappeared, and that there is still some multipeaked structure in $S^{(M)}(Q,\omega)$ at about 10 eV for $f=0.15$, and 11 eV for $f=0.5$. The multipeaked structure in $\Xi(E)$ for the modified SCIB model is smaller in size and shifted to a higher energy, in comparison with the corresponding peaks in the standard SCIB model. Also, the shift to higher energy increases as f increases.

Finally, we can expect that the effects of nonlocality will become smaller as the sphere radius a decreases, since $\epsilon_l(k,\omega)$ depends on k through the combined variable $\rho=ka$. Therefore, the energy-loss spectrum found for either SCIB model should approach the local energy-loss spectrum as $a\rightarrow 0$. Also, the effects of nonlocality should become smaller as the impact parameter z_0 increases. However, since the total strength of the energy-loss spectrum also decreases, the limit of large impact parameter is probably of little interest.

In conclusion, we have shown that the surface region of the system has a strong influence on the energy-loss spectrum. In order to take account of the surface region, we have constructed a modified SCIB model which corrects some of the defects of the standard SCIB model. However, the model is still an approximate theory since it is based on a mean-field approximation and does not treat the correlations of sphere positions near the surface correctly. Also it should be noted that the model is applicable only if there is a planar interface (at $z=0$) between the host material 2 and the vacuum region, with the spherical particles contained entirely within the host material. In fact, depending on how the interface is formed, the surface of the host material might be rough, the spherical particles might penetrate into the vacuum region beyond the $z=0$ plane, so the outermost particles would be only partially embedded in the host, or the portions of those particles that penetrate into the vacuum region might simply be removed, giving nonspherical particle shapes. To treat any of these situations one would have to go considerably beyond the models we have presented.

IV. CONCLUSIONS

In previous work it has been shown that when fast electrons pass through a disordered sample consisting of spherical inclusions at random positions in a host material, electron energy-loss spectroscopy in the valence electron region ($0<E<40$ eV) can be useful for providing structural information, such as the size and volume fraction of the inclusions. However, since the fast electrons can damage the sample, it is of interest to develop a theory of energy loss for electrons traveling parallel to and outside the interface of a semi-infinite system of random spherical inclusions, with the hope that structural information can be obtained using a distant electron beam which does little damage to the sample.

In this work we calculate the energy-loss spectrum of the semi-infinite disordered system starting with models of an infinite disordered system represented by an effective nonlocal dielectric response function $\epsilon_l(k,\omega)$. An important ingredient in the theory is the surface response function $g(Q,\omega)$

of the half space, since the energy-loss spectrum is related to an integral over Q of Im $g(Q,\omega)$. The problem to be solved is how to calculate the half-space response function $g(Q,\omega)$ from the bulk dielectric function $\epsilon_l(k,\omega)$. Although this calculation is, in principle, not possible, we have considered three models which allow an approximate calculation to be performed.

In the first model a local $(k=0)$ limit is used for the bulk dielectric function. In this limit the bulk dielectric function reduces to the well-known Maxwell-Garnett dielectric function, and the calculation of the surface response function is trivial. We determine the energy-loss spectrum for a system of random aluminum spheres in the half space, with vacuum as the host material. We find a single energy-loss peak, associated with the dipolar resonant mode of the spheres. The position of the peak depends on the volume fraction of spheres, and is independent of the sphere radius.

The second model is the semiclassical infinite barrier (SCIB) model, which has previously been applied to find the surface response function of homogeneous nonlocal media. The nonlocal dielectric function of the infinite medium has many resonances associated with both dipole and higher-multipole interfacial modes which lie below the plasma frequency, and a bulk mode at the plasma frequency, which arises from those electrons which pass through the spheres. The energy-loss peaks associated with these modes also appear in the half-space energy-loss spectrum, but the peaks are shifted to energies lower than those in the infinite medium.

The third model is a modified SCIB model, in which we introduce information about the spatial distribution of the spherical inclusions near the surface. It is well known that the standard SCIB model does not represent the surface region adequately, so the intent of this model is to partially correct this deficiency. We first eliminate the bulk mode, arguing that the electrons do not pass through the spherical inclusions. We also modify the strengths of the interfacial modes so that their total strength is consistent with the distribution of spheres near the surface. A simple model for this distribution of spheres is derived by assuming that the spheres cannot penetrate the nominal surface plane, but that otherwise their centers are randomly located. The modified SCIB model gives an interfacial loss peak structure which has both a reduced strength and width, compared to the standard SCIB model.

ACKNOWLEDGMENTS

Part of this work was done at the Cavendish Laboratory, Department of Physics, University of Cambridge. We are grateful to A. Howie, J. Rodenburg, and other members of the Microstructural Physics Group for their hospitality and for making the facilities of the laboratory available to us. We acknowledge interesting discussions with P. M. Echenique, A. Rivacoba, and J. Aizpurua. R.G.B. acknowledges the financial support of Dirección General de Asuntos del Personal Académico of Universidad Nacional Autónoma de México through Grant Nos. IN-102493 and IN-104195. C.I.M. acknowledges the support of Dirección General de Intercambio Académico of Universidad Nacional Autónoma de México and Fundación UNAM, A.C. through ''Reconocimiento a estudiantes distinguidos de la UNAM.'' Ames Laboratory is operated for the U.S. Department of Energy by Iowa State University under Contract No. W-7405-Eng-82.

APPENDIX A: STRENGTHS AND LOCATION OF THE MODES

In this appendix we quote the formulas for the strengths C_b and C_s, and location n_s of the modes which appear in the spectral representation of $\epsilon_l(k,\omega)$ given by Eq. (2) and derived in Ref. 3. The bulk strength is given by

$$C_b=1-3\sum_{l=1}^{\infty} l(2l+1)\left[\frac{j_l(\rho)}{\rho}\right]^2, \tag{A1}$$

where $\rho=ka$. The strengths of the surface modes are

$$C_s=3\sum_{ll'} \sqrt{ll'(2l+1)(2l'+1)}\frac{j_l(\rho)\, j_{l'}(\rho)}{\rho^2}U_{ls}U_{l's}, \tag{A2}$$

where U_{sl} is a unitary matrix which diagonalizes the matrix $H_{ll'}$, i.e.,

$$\sum_{ll'} U_{sl}^{-1}H_{ll'}U_{l's'}=n_s\delta_{ss'}, \tag{A3}$$

and the matrix $H_{ll'}$ is given by

$$H_{ll'}=\frac{l}{2l+1}\delta_{ll'} +3f\sqrt{\frac{ll'}{(2l+1)(2l'+1)}}\frac{(l+l')!}{l!(l')!}\left(\frac{1}{2}\right)^{l+l'-2} \times\frac{j_{l+l'-1}(2\rho)}{2\rho}. \tag{A4}$$

In these equations, $j_\nu(x)$ represents the spherical Bessel function of order ν.

APPENDIX B: DERIVATION OF THE FORMULA FOR $\Xi(E)$

In this appendix we derive the expression for $\Xi(E)$ given in Eq. (7). We assume that the electrons have sufficiently high energy that they travel on a trajectory which deviates only slightly from a straight line and that their energy change is very small compared to the initial energy. Taking the coordinate system defined in Sec. II, we consider an electron of charge $-e$ traveling along a trajectory given by $x=0$, $y=v_I t$, $z=-z_0$ above the half space $(z>0)$ occupied by the system. The energy loss of the electron as it moves a distance dy is given by the negative work done by force on the electron $dW=-F_y\, dy=eE_y\, dy$, where E_y is the induced electric field acting on the electron. Therefore, the energy loss per unit length is

$$\frac{dW}{dy}=-e\left.\frac{\partial\phi^{\rm ind}}{\partial y}\right|_{x=0,\, y=v_I\, t,\, z=-z_0}. \tag{B1}$$

We can find an expression for the induced potential $\phi^{\rm ind}$ in Eq. (B1) by starting with the external charge density of the electron $\rho^{\rm ext}(\mathbf{r},t)=-e\ \delta(x)\ \delta(y-v_I t)\ \delta(z+z_0)$, which has the $t\rightarrow\omega$ Fourier transform

$$\rho^{\rm ext}(\mathbf{r},\omega)=-(e/v_I)\ \delta(x)\ \delta(z+z_0)\ e^{i\omega y/v_I}. \tag{B2}$$

One can then use Coulomb's law to write an expression for the external potential $\phi^{\rm ext}(\mathbf{r},\omega)$. After a trivial integration over z, the remaining integral over x and y is in the form of a convolution. Writing $\mathbf{Q}=(k_x,k_y)$, one can express $\phi^{\rm ext}(\mathbf{Q},z,\omega)$, the two-dimensional Fourier transform of $\phi^{\rm ext}(\mathbf{r},\omega)$, as the product of two Fourier transforms. The result is $\phi^{\rm ext}(\mathbf{Q},z,\omega)=\phi^{\rm ext}(\mathbf{Q},\omega)\ e^{-Qz}$ for $z>-z_0$, where

$$\phi^{\rm ext}(\mathbf{Q},\omega)=-e\frac{(2\pi)^2}{Q}\ \delta(\omega-k_y v_I)\ e^{-Qz_0}. \tag{B3}$$

Using Eq. (B3) in the relation between the external and induced potential given by Eq. (8), followed Eq. (9) to find $\phi^{\rm ind}(\boldsymbol{\rho},z,\omega)$, and an $\omega\rightarrow t$ Fourier transform to give $\phi^{\rm ind}(\boldsymbol{\rho},z,t)$, which is then substituted into Eq. (B1), one gets

$$\frac{dW}{dy}=-\frac{e^2}{v_I^2}\int_{-\infty}^{+\infty}\frac{d\omega}{2\pi}\ \omega\int_{-\infty}^{+\infty}\frac{dk_x}{Q}\ i\ g(Q,\omega)\ e^{-2Q\,z_0}, \tag{B4}$$

where $Q=\sqrt{k_x^2+(\omega/v_I)^2}$. Now one can use the relation $g(Q,-\omega)=g^*(Q,\omega)$ in order to rewrite Eq. (B4) as

$$\frac{dW}{dy}=\frac{2e^2}{\pi v_I^2}\int_0^{\infty}\omega\ d\omega\ \int_0^{\infty}\frac{dk_x}{Q}\ {\rm Im}\,[g(Q,\omega)]\ e^{-2Q\,z_0}. \tag{B5}$$

The probability per unit path length, per unit energy $d^2P/dl\ dE$ of an electron losing energy $E=\hbar\omega$ is defined by

$$\frac{dW}{dy}=\int_0^{\infty}dE\ E\ \frac{d^2P}{dl\ dE}. \tag{B6}$$

Combining Eqs. (B5) and (B6) one gets Eqs. (6) and (7).

APPENDIX C: LOCATION AND STRENGTH OF THE EFFECTIVE MODE

Here we use two sum rules to determine the location and strength of the effective mode used in the calculation. The first sum rule is given in Eq. (4):

$$C_b+\sum_s\ C_s=1,$$

and assures that the sum of the strengths of all the modes is always conserved. If we now replace the modes with $s>6$ with a single ''effective'' mode, the strength of this effective mode $C_{\rm eff}$ was chosen as

$$C_{\rm eff}=1-C_b-\sum_{s=1}^{6}\ C_s \tag{C1}$$

in order to fulfill the sum rule. The location n_s of the modes with $s>6$ lies between $n_6^0=6/13\approx 0.46$ and $n_\infty^0=0.5$ and they show a very weak dispersion; i.e., their location is almost independent of ka. Therefore we choose, for simplicity, the location $n_{\rm eff}$ of the effective mode as a constant halfway between n_6^0 and n_∞^0, that is, $n_{\rm eff}=0.48$. In order to check that this choice is adequate, a second sum rule has to be satisfied,[3]

$$\sum_s\ C_s n_s=F(\rho;f)\equiv\sum_{ll'}\ 3\sqrt{ll'(2l+1)(2l'+1)}\times\rho^{-2}\ j_l(\rho)\ j_{l'}(\rho)\ H_{ll'}, \tag{C2}$$

where $H_{ll'}$ is the matrix given in Eq. (A4). Therefore, our values of $C_{\rm eff}$ and $n_{\rm eff}$ should satisfy the equation

$$C_{\rm eff}\ n_{\rm eff}+\sum_{s=1}^{6}\ C_s n_s-F(\rho;f)=0. \tag{C3}$$

We have checked that for $f=0.5$, the left-hand side of Eq. (C3) is always less than 2×10^{-3}. The same happens for $f=0.15$, except in the interval $0\leqslant ka\leqslant 2$, where the left-hand side of Eq. (C3) can be at most 1.75×10^{-2}.

[1] A. Howie and C. A. Walsh, Radiat. Eff. Defects Solids **117**, 169 (1991).

[2] A. Howie and C. A. Walsh, Microsc. Microanal. Microstruct. **2**, 171 (1991).

[3] R. G. Barrera and R. Fuchs, Phys. Rev. B **52**, 3256 (1995).

[4] R. Fuchs, R. G. Barrera, and J. L. Carrillo, Phys. Rev. B **54**, 12 824 (1996).

[5] R. Fuchs, C. I. Mendoza, R. G. Barrera, and J. L. Carrillo, Physica A **241**, 29 (1997).

[6] J. B. Pendry and L. M. Moreno, Phys. Rev. B **50**, 5062 (1994).

[7] J. B. Pendry and A. MacKinnon, Phys. Rev. Lett. **69**, 2772 (1992).

[8] R. Nuñez, P. M. Echenique, and R. H. Ritchie, J. Phys. C **13**, 4229 (1980).

[9] The spectral representation in Eq. (2) can also be written in a symmetric form where media 1 and 2 appear on the same footing, so there are separate terms for bulk modes in media 1 and 2 as well as terms corresponding to interfacial modes. This symmetric representation is given in Eqs. (8)–(11) of Ref. 4.

[10] P. M. Echenique and J. B. Pendry, J. Phys. C **8**, 2936 (1975).

[11] K. L. Kliewer and R. Fuchs, Phys. Rev. **172**, 607 (1968).

[12] R. Fuchs and R. G. Barrera, Phys. Rev. B **24**, 2940 (1981).

[13] D. L. Johnson and P. R. Rimbey, Phys. Rev. B **14**, 2398 (1976).

[14] D. R. Penn and P. Apell, J. Phys. C **16**, 5729 (1983).